

## A region of the coronavirus infectious bronchitis virus 1a polyprotein encoding the 3C-like protease domain is subject to rapid turnover when expressed in rabbit reticulocyte lysate

K. W. Tibbles,<sup>1</sup> I. Brierley,<sup>1</sup> D. Cavanagh<sup>2</sup> and T. D. K. Brown<sup>1\*</sup>

<sup>1</sup>Division of Virology, Department of Pathology, University of Cambridge, Tennis Court Road, Cambridge CB2 1QP and <sup>2</sup>Institute for Animal Health, Compton Laboratory, Newbury RG20 7NN, UK

In order to investigate the mechanisms involved in the processing of infectious bronchitis virus polyproteins, several candidate regions of the genome have been cloned and expressed *in vitro*. During these studies it was observed that the translation product encoded by one of these clones (pKT205) was poorly expressed. Biochemical and genetic analyses revealed that the basis for the poor expression was a post-translational event involving ubiquitination of the protein and degradation by an ATP-dependent system operating in the reticulocyte lysate used for the *in vitro* expression. Two

independently acting regions which conferred instability were identified, one of which mapped to the predicted 3C protease domain, contained within the 5' end of the clone, while the other, more C-terminal region, was effective in conferring instability upon a heterologous protein to which it had been transferred. These regions may influence the stability of the authentic viral protein(s) *in vivo* and hence allow for the control of their expression and/or function at the level of proteolysis by cellular protease(s).

### Introduction

Coronaviruses employ several mechanisms in order to co-ordinate expression of the linear arrangement of genes from their large positive-sense ssRNA genomes. In the case of avian infectious bronchitis virus (IBV), the mechanisms so far identified are: (i) subgenomic messenger RNA production; (ii) ribosomal frameshifting; (iii) internal initiation of translation; and (iv) polyprotein expression and processing (Brown & Brierley, 1995). This last feature is shared with many other positive-strand viruses such as picornaviruses and flaviviruses, but has been studied much less extensively in coronaviruses.

Coronavirus replication must initiate, upon entry of the genomic RNA into permissive cells, with translation of the input RNA to produce the viral RNA-dependent RNA polymerase. This activity copies the genomic RNA into a negative-sense template which is then transcribed, producing a nested set of 3' co-terminal transcripts from which further viral protein synthesis proceeds (reviewed

in Spaan *et al.*, 1988; Lai, 1990). In the case of IBV the transcripts include the full-length genomic RNA, mRNA1 of 27.6 kb (Bournsnell *et al.*, 1987) and five subgenomic RNAs (Stern & Kennedy, 1980) designated mRNAs 2–6 in descending order of size (Cavanagh *et al.*, 1990). Each transcript in the series specifies one of the genes in the linear genome arrangement by virtue of the portion of genomic sequence at its 5' terminus that is not present in the next smallest transcript (Stern & Sefton, 1984). Most of the coding potential of the IBV genome (approximately 70%) is contained within two large overlapping open reading frames, ORFs 1a and 1b, present in the 'unique' region, comprising gene 1, located at the 5' end of mRNA1 (Bournsnell *et al.*, 1987). The remaining (eight) ORFs, including those of all structural proteins identified to date, are encoded within the remaining 3' end of the genome and are expressed from the subgenomic mRNAs. It would seem that non-structural proteins, including the polymerase function(s), predominate in gene 1. Although a number of replication-associated activities have been predicted to be encoded by mRNA1 (Gorbalenya *et al.*, 1989), little is known concerning the identity or function of the ORF 1a and 1b products.

The region of overlap between ORFs 1a and 1b is only 42 nucleotides, with ORF 1b occupying the –1 frame

\* Author for correspondence. Fax +44 1223 336926. e-mail tdkb@mole.bio.cam.ac.uk

with respect to ORF 1a. Data have been reported demonstrating ribosomal frameshifting between ORFs 1a and 1b (Brierley *et al.*, 1987, 1989) which allows read-through of the 1a stop codon and therefore expression of 1b (which does not have its own subgenomic mRNA) as a fusion product 1a/1b. Thus, translation of gene 1 would result potentially in a stopped product (from ORF 1a) of 441 kDa and a read-through product (from 1a/1b) of 741 kDa. Similar arrangements have been demonstrated for other coronaviruses including mouse hepatitis virus (MHV; Lee *et al.*, 1991) and human coronavirus (HCV) strain 229E (Herold *et al.*, 1993). These large precursors undergo post- or co-translational processing in order to generate the mature non-structural proteins associated with viral replication. Attempts to identify and relate precursors and processed products in IBV-infected cells using monospecific antisera met with some success (Brierley *et al.*, 1990). A number of viral polypeptides were detected, although the low levels of mRNA1-encoded polypeptides present in infected cells and an incomplete range of reactive antisera have made further analyses difficult. *In vivo* processing data have also been reported for MHV (Denison *et al.*, 1992), where evidence of multiple proteolytic events was presented. These technical difficulties and the complexity of the events involved make the development of *in vitro* systems desirable. Two potential protease domains have been identified within the IBV ORF 1a sequence (Gorbalenya *et al.*, 1989), one of which (3CLP) shows high similarity to the picornavirus 3C-like proteases and is common to all coronaviruses so far analysed. Using a vaccinia virus-T7 expression system, this domain has recently been shown to exhibit authentic processing activity when appropriate regions of ORF 1 are expressed (Liu *et al.*, 1994). Until recently, the only *in vitro* processing activity reported had been for the MHV papain-like protease (PLP1), located towards the 5' end of the genome and apparently absent from IBV. In the case of MHV, a 28 kDa polypeptide (p28) synthesized in virus-infected cells (Denison & Perlman, 1987) has been shown to be derived from the N terminus of a larger precursor when expressed from the 5' end of ORF 1a *in vitro* (Denison & Perlman, 1986; Soe *et al.*, 1987). This cleavage is mediated by PLP1 (Baker *et al.*, 1989, 1993). Two recent reports have now described *in vitro* processing activities for cloned 3C-like proteases of both MHV (Lu *et al.*, 1995) and HCV (Ziebuhr *et al.*, 1995).

Our present studies concern the characterization of the mechanism(s) involved in IBV polyprotein processing by examination of the *in vitro* expression of gene 1 from cloned viral sequences corresponding to ORFs 1a and 1b. Given that the sizes of ORFs 1a and 1b represent severe challenges to expression by the *in vitro* transcription and translation systems currently available, and to

simplify interpretation, we sought initially to express several smaller overlapping clones covering the 1a/1b region using bacteriophage T7 RNA polymerase and rabbit reticulocyte lysate. Here we report data on the expression of one of these clones which suggest that a region of ORF 1a encoding the 3C-like protease domain is a target for the ubiquitin-mediated ATP-dependent degradation system present in the lysate. This finding is discussed in the light of recent reports in which a number of other virus groups appear to use this cellular system to control protein expression/function and particularly in regard to an emerging pattern of metabolic instability amongst 3C-like viral proteases.

## Methods

**Plasmids.** The IBV expression plasmids described in this report were constructed from cDNA clones generated originally by Bournsnel *et al.* (1987). The relevant cDNA fragments were purified from their vector backgrounds and cloned into a T7 transcription vector pKT0/NS1 (Liu *et al.*, 1994). This vector provides an efficient eukaryotic translation initiation module to allow expression of DNA sequences introduced at appropriate in-frame downstream restriction sites. A *StuI*-*PstI* fragment (clone 205), comprising IBV sequence information from nucleotide (nt) position 8693 to approximately 10930 was introduced in-frame into pKT0/NS1, at the *EcoRV* and *PstI* restriction sites, to yield pKT205. A similarly-sized *NsiI*-*PstI* fragment (clone BP5) corresponding to the IBV sequence from nt 10752 to approximately 12600 was introduced in-frame at the *PstI* site of pKT0/NS1 to produce pKTBP5. Construction of these plasmids has been detailed elsewhere (Liu *et al.*, 1994).

A frameshift mutant of the 205 sequence (pKT205 $\Delta$ C<sup>Nco</sup>) was obtained by digestion of pKT205 with *NcoI* followed by end-repair and religation. The introduction of the additional 4 bp (at the unique *NcoI* site at nt 10118) results in a frameshift of translation such that a stop codon is encountered 35 bases downstream. A larger C-terminal deletion plasmid was created by excision of a *NsiI* (nt 9370)-*PstI* (polylinker) fragment from the parental pKT205 plasmid to yield pKT205 $\Delta$ C<sup>Nsi</sup>. The N-terminal deletion construct pKT205 $\Delta$ N<sup>Pvu</sup> was constructed by recloning the 205 sequence between the *PvuII* site (nt 9911) and the *PstI* site (polylinker) into *EcoRV*/*PstI*-digested pKT0/NS1 vector.

Plasmids pKT1<sup>+</sup> and pKT1/205 were obtained as follows: a DNA fragment corresponding to influenza virus segment 2, encoding PB<sub>1</sub>, was excised from pAPR206 (Young *et al.*, 1983) by digestion with *EcoRI*, end-repaired and introduced into *PvuII*-digested pKT0 (Liu *et al.*, 1994) to produce pKT1<sup>+</sup>. This plasmid was digested with *EcoRV* (nt 2156) and *AvaI* (polylinker) to allow insertion of a *XmnI* (nt 10184)-*AvaI* (polylinker) fragment from pKT205 encoding the C-terminal end of the 205 protein. Oligonucleotide-directed mutagenesis was employed to restore the *EcoRV* site and the reading frame at the PB<sub>1</sub>-205 junction such that the two ORFs were in the same reading frame and translationally fused. A deletion of the C-terminal half of the PB<sub>1</sub> sequence within pKT1/205 was performed to create pKT1 $\Delta$ C/205. This was achieved by the mutagenic insertion of an in-frame *EcoRV* site 1 kb upstream of the existing *EcoRV* site, followed by excision of the intervening sequence by *EcoRV* digestion and religation of the plasmid. All cloning steps were confirmed by restriction enzyme digestion and dideoxynucleotide sequencing of cloning junctions. The control construct (for energy-dependent degradation), expressing a human papillomavirus type 16 (HPV-16) E6-cyclin chimeric protein,

was kindly provided by T. Crook (Raine Institute, King's College, University of London, London, UK).

**Mutagenesis.** The pKT0/NS1 expression vector carries the packaging signals for the filamentous bacteriophage  $\phi$ 1 (Dotto *et al.*, 1981) enabling the rescue of ssDNA following superinfection of bacterial cells (bearing the plasmid) with phage R408 (Russel *et al.*, 1986). Oligonucleotide-directed mutagenesis (Kunkel, 1985) was carried out as described by Brierley *et al.* (1989).

**In vitro transcription and translation.** Plasmid DNA was linearized at an appropriate restriction site downstream of the IBV sequence (unless stated otherwise) prior to transcription by T7 RNA polymerase as described (Brierley *et al.*, 1987). RNA was purified by spun-column chromatography, concentrated by ethanol precipitation and translated in an mRNA-dependent rabbit reticulocyte lysate (Promega) containing [<sup>35</sup>S]methionine (0.75 mCi/ml). Alternatively, a coupled transcription-translation system was used (Craig *et al.*, 1992). In this protocol, MgCl<sub>2</sub> and NTPs were added to the lysate at approximately 5 mM and 1 mM, respectively, and reactions initiated by the addition of undigested plasmid DNA and T7 RNA polymerase. Reactions were terminated (typically after 1 h) by incubation with 1 × translation stop buffer (2 mM-L-methionine, 500 µg/ml cycloheximide, 50 mg/ml DNase 1 and 50 mg/ml RNase A) for 15 min at 30 °C. Expression of the E6-cyclin protein was achieved using the SP6-qualified wheatgerm transcription-translation system from Promega. Polypeptide products were separated on 15% polyacrylamide-SDS gels (Hames, 1981) and visualized by autoradiography (unless stated otherwise).

**Protease assays.** Assays (10 µl) were performed typically using 1 µl of a completed translation reaction, 1 µl of 10 × translation stop buffer and 5–8 µl of reticulocyte lysate (unless stated otherwise). Incubation was carried out for 1 h at 30 °C, or up to 3 h where indicated. The multicatalytic protease inhibitor MG132 was a generous gift from F. Baleux and R. T. Hay (School of Biological and Medical Sciences, University of St Andrews, St Andrews, UK) and was used at 50 µM. When utilized, adenosine-5'-O-(3-thiotriphosphate) (γ-S-ATP; 4 mM final concentration) was added to the lysate prior to addition to target translates. Reactions were terminated by boiling in SDS sample buffer prior to electrophoresis.

**Preparation of labelled ubiquitin and ubiquitin complexes.** A modified version of ubiquitin was kindly supplied by A. Klotzbücher (Imperial Cancer Research Fund, South Mimms, Hertfordshire, UK). This protein has been engineered so as to contain an N-terminal peptide sequence that acts as a substrate for phosphorylation by the catalytic subunit of protein kinase A (Boehringer Mannheim). Phosphorylation using [γ-<sup>32</sup>P]ATP as a phosphate donor was carried out at 37 °C for 15 min following the manufacturer's guidelines. Free label was removed by gel filtration. Approximately 1 µg of labelled ubiquitin was incubated alone or in the presence of 5 µl of reticulocyte lysate for 15 min at room temperature to allow incorporation into multiubiquitin complexes with endogenous lysate proteins. Alternatively, labelling was carried out after complex formation using lysate that had been incubated alone or in the presence of the engineered ubiquitin.

**Ubiquitin depletion of reticulocyte lysate.** Aliquots of lysate (100 µl) were diluted 25-fold with buffer (10 mM-Tris-HCl pH 7.4, 1 mM-MgCl<sub>2</sub>) and concentrated back to the original volume using a centricon 10 filtration unit (Amicon). Lysates were resupplemented with ATP (to 1 mM) and creatine phosphate (to 10 mM) and used in a ubiquitination assay as follows: reactions were carried out as described for the protease assay above except that depleted lysate, supplemented or unsupplemented with purified bovine ubiquitin (5 µg; Sigma), was used in place of untreated lysate. Incubation was restricted to 15 min (at room temperature) to prevent significant degradation of the ubiquitin-target complexes.

## Results

### *Observations that reveal two potential degradation signals within the 205 protein*

The 205 clone was chosen for expression analysis as it encodes the predicted 3C-like protease domain as well as several potential cleavage sites (Gorbalenya *et al.*, 1989) and was expected therefore to provide the basis for *in vitro* processing studies. *In vitro* expression of the pKT205 plasmid was predicted to yield a 75 kDa primary translation product which, as shown in Fig. 1(a) lane 2, could be detected although in comparatively low abundance. The predominant products of translation were truncated forms, most of which probably arose from premature termination events since 3' truncation of the RNA did not affect their relative mobilities (i.e. they share common N-termini; see Fig. 2a, lanes 3, 4 and 5). Attempts to investigate the possibility that autoproteolysis of the 205 protein was occurring were hampered by the complexity of the translation pattern (released 3C is expected to migrate at approximately 35 kDa); synthesis in the presence of a range of water soluble protease inhibitors did not reveal significant differences in the pattern obtained (data not shown). Another feature of the translation pattern for the 205 clone was the incorporation of significant amounts of radiolabel into heterogeneous high molecular mass products which formed a smear extending from around 50 kDa to the top of the separating gel, where a proportion appeared unable to penetrate. This pattern was unaffected by the RNase treatment of sample preparation. The appearance of high molecular mass species contrasted strongly with the pattern of protein synthesis from other regions of gene 1, as shown by the example in Fig. 1(a), lane 1. This pattern was produced from the expression of the BP5 sequence, which lies adjacent to and downstream from the 205 region (though overlapping by some 200 bases) in the IBV genome. Two translation products of 60 and 70 kDa were obtained which were of the sizes expected to result from translation termination and frameshifting events at the 1a/1b boundary, contained within the 3' end of the BP5 clone. There were several background bands but no evidence of significant amounts of high molecular mass heterogeneous material.

A time-course analysis of the expression of the 205 protein was performed (Fig. 1b) to examine whether the poor level of full-length 205 protein resulted from poor expression *per se* or from instability. Full-length product was detectable by 30 min and increased for a further 30 min before declining, a pattern also exhibited by some of the shorter products. No accumulation of shorter products was observed to suggest that processing was occurring. Throughout this latter period, the high molecular mass material was seen to accumulate at the

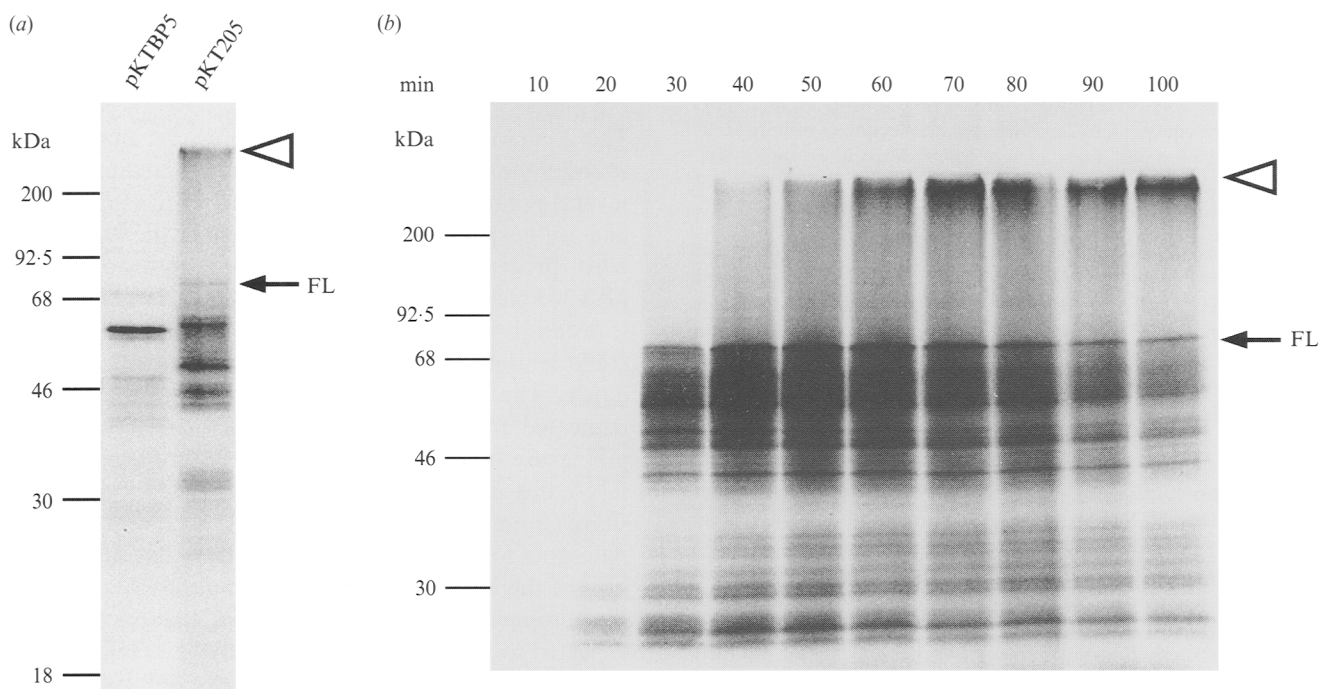


Fig. 1. (a) Comparison of the *in vitro* translation products produced from plasmids pKTBP5 and pKT205. Separate transcription and translation reactions (60 min) were performed and the  $^{35}\text{S}$ -labelled products (2  $\mu\text{l}$ ) were separated on a 15% polyacrylamide-SDS gel. Radiolabelled polypeptides were detected by autoradiography. The positions and molecular masses of protein size standards (Amersham) are shown on the left. The closed arrow indicates the position of the expected full-length (FL) 205 product and the open arrow marks the top of the separating gel. (b) Time-course analysis of the accumulation of [ $^{35}\text{S}$ ]methionine-labelled products from coupled *in vitro* transcription and translation of pKT205. Reactions (25  $\mu\text{l}$ ) were performed as described in the text and samples (2  $\mu\text{l}$ ) were removed at the intervals (min) indicated and mixed immediately with gel sample buffer. Polypeptide products were separated on a 15% polyacrylamide-SDS gel and detected by autoradiography.

top of the gel, an observation consistent with the conversion of free nascent protein into these other forms. Accumulation of the high molecular mass material appeared dependent upon completion, or near completion, of the full-length translation product. The behaviour of the 205 protein is suggestive of the multiubiquitination that normally occurs prior to degradation of such targeted proteins by an energy-dependent 26S cellular protease complex (Hershko *et al.*, 1984). Since the 205 clone encodes the predicted 3C-like protease domain of IBV, this observation suggested a correlation with the observed low *in vitro* stability of the encephalomyocarditis virus (EMCV) 3C protease, which has been attributed to energy-dependent proteolysis (Oberst *et al.*, 1993).

We tested the importance of the C terminus in determining the behaviour of the 205 protein by translation of a series of 3'-terminally truncated RNA transcripts obtained by run-off transcription of appropriately linearized pKT205 plasmid. As revealed in Fig. 2(a), primary translation products of the expected sizes were obtained from the corresponding truncated RNAs and there was no evidence for autocatalytic

processing, as had been anticipated. This strongly implicates the C terminus of the full-length 205 protein (beyond the *HincII* site) in determining its fate. We had considered the possibility that the reduced expression of the 205 protein may have arisen as a result of inefficient initiation of translation, perhaps caused by an interaction between the initiation start site and the 3' end of the RNA produced from the full-length 205 construct. However, when we expressed a variant 205 plasmid, pKT205 $\Delta\text{C}^{\text{Nco}}$  (Fig. 3a, lane 1), in which a frameshift mutation had been introduced at the unique *NcoI* site (position 10118, see Methods), translation was relatively efficient, producing a translation product of the expected size. In pKT205 $\Delta\text{C}^{\text{Nco}}$ , the C terminus of 205 is not expressed, since the introduced frameshift mutation brings a nonsense codon into register some 11 amino acids downstream of the introduced frameshift. Yet an almost identical RNA sequence is retained, strongly supporting the notion that the poor levels of 205 protein were due to a post-initiation event. If these levels are caused by degradation of ubiquitinated forms, the data would suggest the involvement of the C terminus in targeting. However, the C terminus lies beyond the

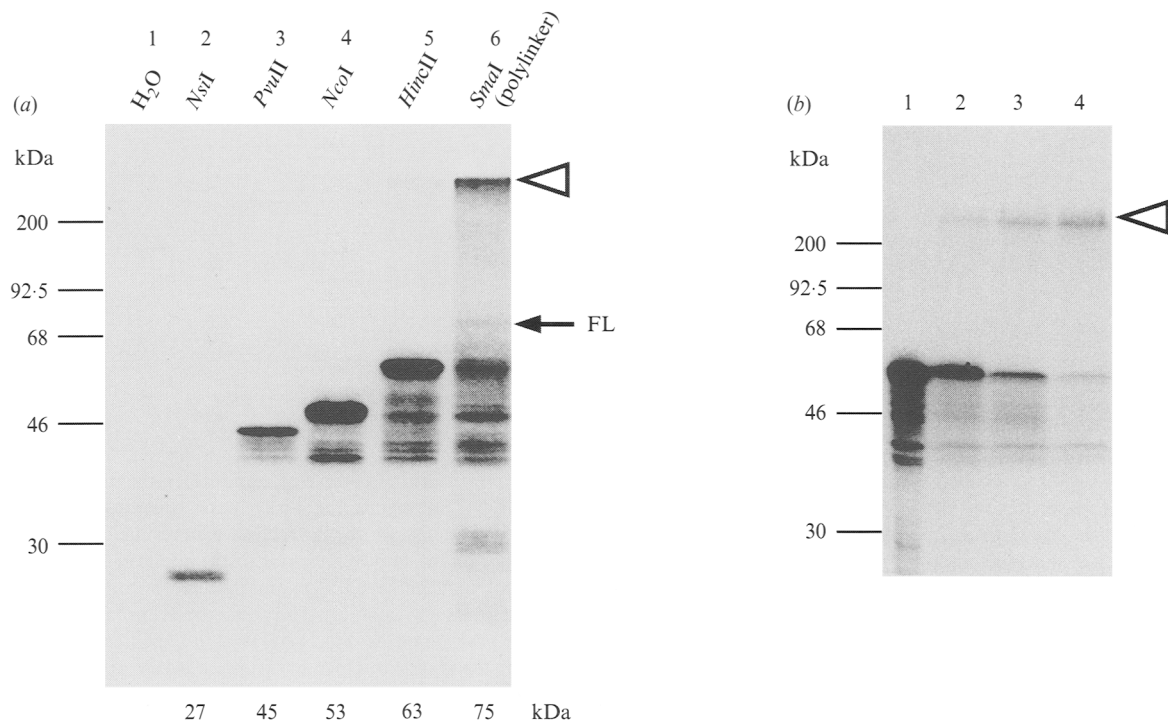


Fig. 2. (a) C-terminal deletion analysis of the 205 translation product. The plasmid pKT205 was linearized at the restriction sites indicated and capped run-off transcripts generated *in vitro* using T7 RNA polymerase. Translations (60 min) were performed in the presence of [<sup>35</sup>S]methionine and the labelled products were analysed by autoradiography following separation on a 15% polyacrylamide-SDS gel. The molecular mass (kDa) of the expected translation product of each transcript is indicated below the corresponding lane. Lane 1 contains a control translation in which water replaced RNA. (b) Analysis of the susceptibility of the *Hinc*II target protein to modification/degradation. Uniform amounts of the completed translation (1  $\mu$ l) were incubated with increasing amounts of fresh reticulocyte lysate as described in Methods. Lanes 1, 2, 3 and 4 are the result of adding 0, 2, 5 and 10  $\mu$ l of fresh lysate, respectively.

predicted 3C protease domain (which resides at the N terminus of the 205 protein) and there was still evidence consistent with some ubiquitination of the *Nco*I and *Hinc*II products (Fig. 2a, lanes 4 and 5; Fig. 3a, lanes 1 and 3) suggesting that a second ubiquitination signal could also be present. As the extent of production of the high molecular mass material was considerably reduced in these translations, it was considered possible that the putative ubiquitination at this second site could be limited by the availability of the necessary components in the lysate. This was tested by incubating the *Hinc*II-truncated translation product with increasing amounts of unprogrammed reticulocyte lysate under conditions where further translation was prevented. As shown in Fig. 2(b), the protein was seen to convert progressively into high molecular mass forms, becoming trapped at the top of the gel. This could not be demonstrated for a metabolically stable control protein (influenza virus PB<sub>1</sub>; see below) indicating the specificity of the process. Also apparent was the loss of a significant amount of the total radiolabelled material in the presence of the higher

amounts of added lysate, suggesting that degradation of some of the protein had occurred. Degradation was confirmed by analysis of TCA-precipitable radiolabelled product over a 2 h period (data not shown).

The possibility that two degradation signals (degrons) exist within the 205 sequence was confirmed by the experiments shown in Fig. 3(a), which were performed to demonstrate the ATP dependence of the instability of the 205 proteins. The target proteins produced from plasmids pKT205 (*Bst*XI-restricted), pKT205 $\Delta$ C<sup>Nco</sup>, pKT205 $\Delta$ C<sup>Nsi</sup> and pKT205 $\Delta$ N<sup>Pvu</sup> were incubated in the presence or absence of excess lysate containing  $\gamma$ -S-ATP. In the presence of this ATP analogue, ubiquitinated proteins accumulate, since  $\gamma$ -S-ATP can substitute for ATP in the ubiquitination reaction but not the consequent degradation reaction (Scheffner *et al.*, 1992). As seen by comparing lanes 1 and 2 of Fig. 3(a), this treatment resulted in the conversion of the pKT205 $\Delta$ C<sup>Nco</sup> product along with most of the incomplete translation products to high molecular mass forms. This was accompanied by stabilization of the high molecular mass

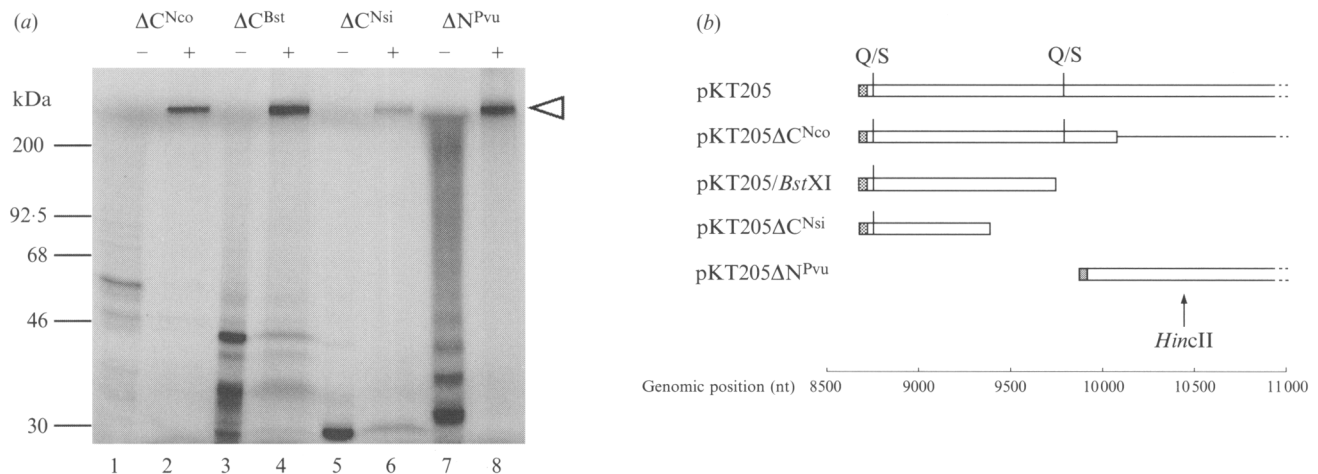


Fig. 3. (a) Result of incubating full-length and deleted 205-derived target proteins (1  $\mu$ l of completed translate) in the presence (+) or absence (-) of excess fresh reticulocyte lysate (5  $\mu$ l) and 4 mM- $\gamma$ -S-ATP. Substrates for assay were generated by coupled transcription-translation of the appropriate plasmid DNA except in the case of the *Bst*XI target protein which resulted from separate transcription and translation reactions. Synthesis was terminated by the addition of stop buffer prior to the addition of fresh lysate. The  $^{35}$ S-labelled products of these incubations were separated on a 15% polyacrylamide-SDS gel and detected by autoradiography. (b) Diagram summarizing the primary structures of the proteins used in the study shown in (a). The predicted 3C protease domain is defined by the two glutamine-serine (Q/S) cleavage sites. Also shown is the position of the *Hinc*II site used in the C-terminal deletion experiments (Fig. 2). The genomic positions of the proteins are indicated by the scale bar. Open bars represent IBV protein sequence while the filled portions at the N-termini represent common sequence donated by the expression vector (corresponding to the first 4 amino acids of influenza virus NS<sub>1</sub> protein). Also depicted as a narrow bar at the C terminus of the  $\Delta$ C<sup>Nco</sup> protein is the untranslated region of the RNA from pKT205 $\Delta$ C<sup>Nco</sup>.

material retained at the top of the gel, suggesting that the degradation (as seen in Fig. 2b) was ATP-dependent. Some laddering of the pKT205 $\Delta$ C<sup>Nco</sup> product was evident, which would be consistent with ubiquitination prior to degradation. The *Bst*XI protein, which also exhibited a defined (RNase-resistant) ladder of protein species (Fig. 3a, lane 3), was also significantly diminished by the addition of excess lysate (lane 4), as was the *Nsi*I protein (compare lanes 5 and 6). An increase in the ubiquitinated forms at the top of the gel could also be detected in each case. The N-terminal deletion protein ( $\Delta$ N<sup>Pvu</sup>, lane 7) which bears the original C-terminal signal (beyond the *Hinc*II site) clearly demonstrated laddering, the spacing of which was consistent with the sequential addition of ubiquitin moieties (of approximately 8 kDa), as expected for a classical ubiquitin ladder (Hough & Rechsteiner, 1986). This pattern was observed when the protein was expressed using separate transcription and translation reactions, so did not represent an artefact of the coupled system. The ladder was converted to high molecular mass products by the addition of excess lysate (lane 8). Similar results were observed when extracts made from Vero cells (a cell type permissive for viral infection) were used (data not shown). It is not clear why the processes of degradation fail to finish without the addition of excess lysate (all incubations were carried out under conditions that

prevent further protein synthesis). One possibility is that of factor limitation within the lysate (we have noted batch variation in the degree of activity), although the addition of purified bovine or yeast ubiquitin did not increase the rate or extent of the reaction(s) (data not shown). An alternative explanation is that only a proportion of the necessary factors potentially involved are free to operate due to regulatory mechanisms.

The primary structures of the proteins used are summarized in Fig. 3(b). The behaviour of the pKT205 $\Delta$ C<sup>Nsi</sup>- and pKT205 $\Delta$ N<sup>Pvu</sup>-derived proteins, which do not overlap, confirms the independent nature of the destabilizing regions. Therefore, two degrons are proposed. The first lies between the N terminus of the 205 protein and the *Nsi*I site and would therefore reside within the N-terminal portion of the predicted 3C domain; the second is bounded by the *Pvu*II site and the C terminus of the 205 protein and would appear to lie beyond the *Hinc*II site, according to the results shown in Fig. 2(a).

#### *Evidence for the involvement of ubiquitin in the modification of target proteins*

The laddering observed during translation of the 205 proteins and their conversion, along with the corresponding 'free' products, to high molecular mass

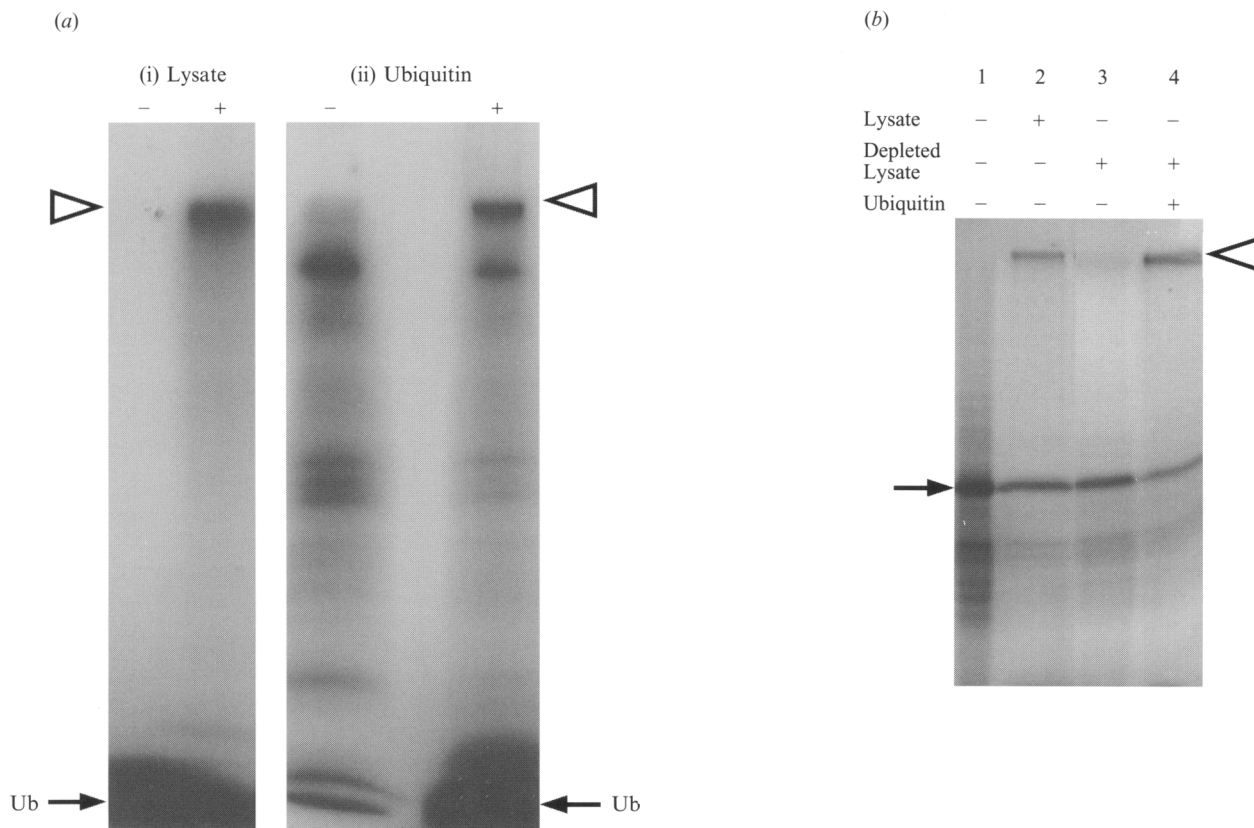


Fig. 4. (a) Demonstration of the incorporation of ubiquitin into high molecular mass complexes.  $^{32}\text{P}$ -labelled ubiquitin (Ub; approximately 1  $\mu\text{g}$ ) was incubated in the presence (+) or absence (-) of 5  $\mu\text{l}$  of reticulocyte lysate for 15 min at room temperature (i). Reactions were terminated by addition of sample buffer and products analysed on a 20% polyacrylamide-SDS gel. In the reciprocal experiment (ii), lysate was incubated with (+) or without (-) unlabelled ubiquitin followed by phosphorylation using [ $\gamma$ - $^{32}\text{P}$ ]ATP and protein kinase A (37  $^{\circ}\text{C}$ , 15 min). The positions of free ubiquitin and the top of the separating gel are indicated by the closed and open arrows, respectively. (b) Ubiquitin-dependent modification of the *BstXI* target protein. One  $\mu\text{l}$  of target *BstXI* protein (closed arrow) was incubated at room temperature for 30 min either alone (lane 1), in the presence of 8  $\mu\text{l}$  of fresh reticulocyte lysate (lane 2), in the presence of depleted lysate (lane 3; see Methods), or in the presence of depleted lysate supplemented with 10  $\mu\text{g}$  of purified ubiquitin (lane 4). Products were analysed as described in (a).

modified forms by the reticulocyte lysate was very suggestive of the multiubiquitination that occurs prior to degradation by the multicatalytic protease. Further evidence for this was provided by the following observations: Fig. 4(a) shows the behaviour of labelled ubiquitin when incubated with reticulocyte lysate. In the presence of lysate (15 min incubation) a proportion of the ubiquitin was seen to become incorporated into high molecular mass material at the top of the gel, presumably as the result of involvement in the ubiquitination of endogenous lysate proteins (compare left and right lanes in each panel). This could be observed whether the ubiquitin was labelled prior to (left panel) or after (right panel) incubation with lysate (some lysate proteins were also labelled in the latter case, but the labelling of these was diminished in the presence of ubiquitin). These reciprocal experiments showed that the appearance of the labelled high molecular mass material was specific to

the inclusion of exogenous ubiquitin, and that the behaviour of ubiquitin closely mirrors that of the 205 proteins.

We were unable to stimulate ubiquitination of target proteins by the addition of purified ubiquitin to translation reactions. But it proved possible to produce a lysate that was severely restricted in its capacity to modify target proteins by removal of much of the free ubiquitin pool using membrane filters with a 10 kDa cut-off (centricon 10 units, Amicon). When lysate so depleted was incubated with target (*BstXI*) protein, modification was at a much reduced level compared to untreated lysate (Fig. 4b, compare lanes 2 and 3). However, supplementation of the depleted lysate with purified ubiquitin (lane 4) resulted in some restoration of the modifying activity. Although it is not certain which other small components of the lysate are removed by this treatment, restoration of modifying activity specifically

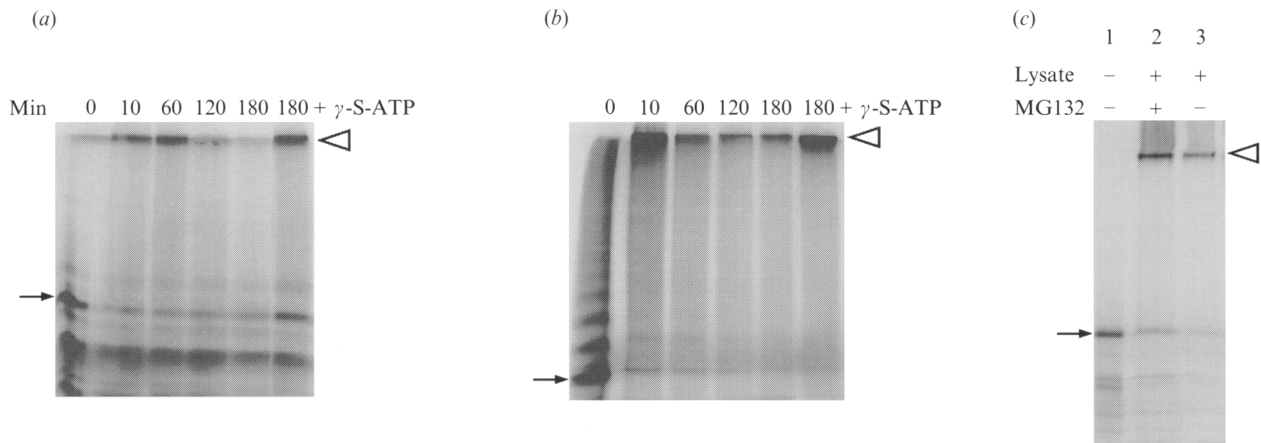


Fig. 5. (a) Energy-dependent degradation of modified *BstXI* target protein. Reactions (50  $\mu$ l) consisted of 10  $\mu$ l of target translate and 40  $\mu$ l of fresh reticulocyte lysate and were carried out at 30 °C. Time-point samples (10  $\mu$ l) were removed at the times indicated, mixed with gel sample buffer and analysed on a 15% polyacrylamide-SDS gel. A parallel reaction containing 4 mM- $\gamma$ -S-ATP was also performed (only the 180 min time-point is shown). The closed arrow indicates the position of the unmodified target protein obtained from translation of the pKT205/*BstXI*-derived RNA, the open arrow corresponds to the top of the resolving gel. (b) Energy-dependent degradation of modified  $\Delta N^{Pvu}$  target protein. The experiment was performed exactly as described for the *BstXI* protein above. The closed arrow indicates the position of the free primary translation product obtained by coupled transcription-translation reactions using the pKT205 $\Delta N^{Pvu}$  plasmid as described in Methods. (c) Inhibition of degradation of modified *BstXI* protein by MG132. Reactions comprised 1  $\mu$ l of target (*BstXI* protein, closed arrow) with (+) or without (-) the addition of 8  $\mu$ l of fresh lysate, in the presence (+) or absence (-) of 50  $\mu$ M-MG132 and were carried out for 2 h at 30 °C. Reactions were terminated by the addition of sample buffer and the products analysed on a 15% polyacrylamide-SDS gel.

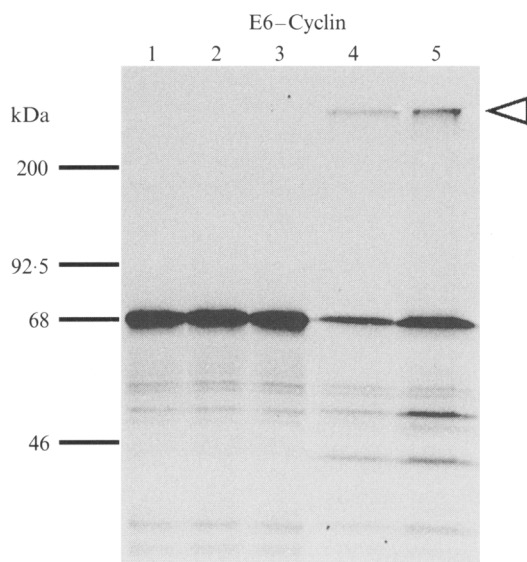


Fig. 6. Demonstration of the energy dependence of modification and degradation of the control E6-cyclin protein synthesized in wheatgerm lysate. Samples (1  $\mu$ l) of completed wheatgerm extract transcription-translation reactions were incubated for 60 min in the absence (lane 2) or presence (lanes 4 and 5) of fresh reticulocyte lysate (8  $\mu$ l) with the omission (lane 4) or addition (lane 5) of 4 mM- $\gamma$ -S-ATP. Also included are unincubated control samples with (lane 3) or without (lane 1) the addition of reticulocyte lysate immediately prior to analysis. Products were separated on a 15% polyacrylamide-SDS gel and visualized by autoradiography.

by purified ubiquitin provides good evidence that the observed modification of the 205 proteins by reticulocyte lysate is due to ubiquitination.

#### Evidence for the involvement of the 26S ATP-dependent protease in the degradation of modified target proteins

As mentioned previously, a characteristic feature of the ubiquitin-mediated ATP-dependent proteolytic system is the sensitivity of the multicatalytic protease to inhibition by  $\gamma$ -S-ATP, while ubiquitination remains refractory to this agent. We investigated the effect of  $\gamma$ -S-ATP upon the degradation of modified target proteins more closely. In Fig. 5(a), where *BstXI* target protein was incubated with excess lysate for the times indicated, modification was seen to occur rapidly within the first 10 min (as shown by the accumulation of label at the top of the gel) and was essentially complete by 60 min. Thereafter, degradation of the high molecular mass material was seen to proceed during the further 2 h of incubation. In contrast, while it could be seen that in the presence of  $\gamma$ -S-ATP modification of the target was unaffected, degradation over the same period was significantly reduced, with a greater proportion of material remaining at the top of the gel. A similar pattern of events was obtained when the  $\Delta N^{Pvu}$  target was used (Fig. 5b). These data demonstrate clearly the ATP

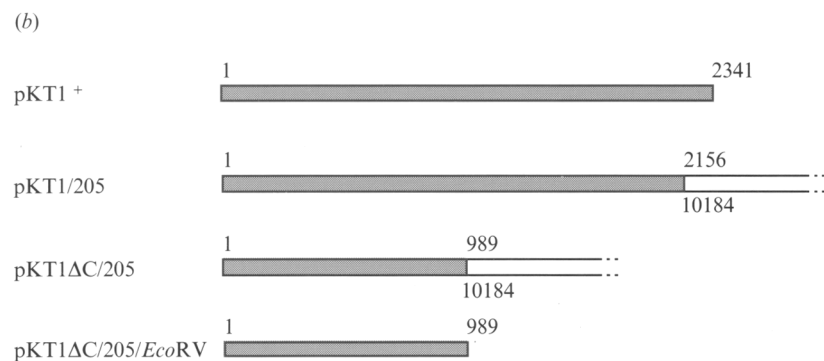
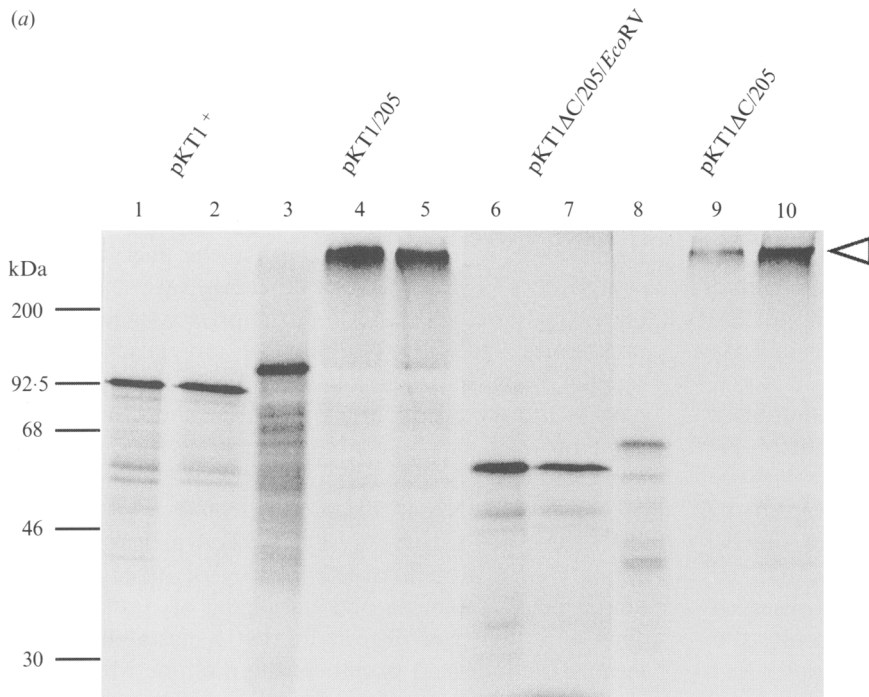


Fig. 7. (a) Comparison of the *in vitro* stabilities of wild-type PB<sub>1</sub> (encoded by pKT1<sup>+</sup>, lanes 1 and 2) and chimeric proteins (encoded by pKT1/205, lanes 3–5; and pKT1ΔC/205, lanes 6–10) in the presence of excess reticulocyte lysate. The experiment was performed essentially as described in Fig. 6. Lanes 1, 3, 6 and 8 contain products resulting from incubation of targets (1 μl) in the absence of fresh lysate. Lanes 2, 4, 7 and 9 show the effect of incubating targets in the presence of 8 μl of fresh lysate. Lanes 5 and 10 show the effects of incubation of targets with excess lysate in the presence of 4 mM-γ-S-ATP. The control pKT1ΔC/205/*EcoRV* product (comprising the N-terminal portion of PB<sub>1</sub> only) was obtained by separate transcription and translation reactions using *EcoRV*-digested pKT1ΔC/205 DNA (lanes 6 and 7). (b) Schematic representation of the proteins used in (a). Influenza PB<sub>1</sub> sequence is represented by the filled bars and that of IBV (205) by the open sections. Nucleotide coordinates are indicated.

dependence of degradation of the modified target proteins, as expected for operation of the ubiquitin-mediated ATP-dependent proteolytic system.

Additional evidence for the involvement of this system was obtained by use of a specific inhibitor of the multicatalytic protease, MG132 (carboxybenzoyl-leu-leu-leucinal; R. Hay, personal communication). In Fig. 5(c), a comparison is shown between the extent of degradation of ubiquitinated *Bst*XI protein (lane 1) in the presence (lane 2) or absence (lane 3) of MG132. It can be seen that the presence of MG132 significantly reduced the extent of degradation of the ubiquitinated target protein over the incubation period.

The behaviour of the 205 proteins is consistent with that established for the control E6-cyclin protein as demonstrated in parallel experiments (Fig. 6). Since ubiquitination of E6 requires association with a 100 kDa

reticulocyte lysate protein (E6-AP) which is absent in wheatgerm extract (Scheffner *et al.*, 1993), unubiquitinated E6-cyclin can be synthesized in wheatgerm extract (lane 1) and subsequently ubiquitinated and degraded by the addition of reticulocyte lysate (lane 4). In the presence of γ-S-ATP, degradation is inhibited as shown by the stabilization of ubiquitinated protein at the top of the gel (lane 5).

#### Further characterization of the C-terminal degron

Partial characterization of the C-terminal degron was carried out in terms of its context specificity. Fig. 7(a) shows the result of transferring the C-terminal region of 205 (downstream from the *Xmn*I site at position 10184) containing the degradation signal to a normally stable heterologous protein, the influenza virus (A/PR/8/34)

PB<sub>1</sub> protein (the primary structures of the proteins are shown in Fig. 7*b*). The wild-type PB<sub>1</sub> protein was completely stable when incubated with excess lysate (Fig. 7*a*, compare lanes 1 and 2) whereas incubation of the PB<sub>1</sub>/205 translation product (lane 3) with excess lysate (lane 4) resulted in complete conversion to the high molecular mass forms. However, the rate of decay would appear to be low, as shown by the similar levels of material remaining (at the top of the gel) either in the absence or presence of  $\gamma$ -S-ATP (compare lanes 4 and 5). Removal of the C-terminal half of the PB<sub>1</sub> protein resulted in a markedly less stable chimeric protein, as shown by comparing the high molecular mass material remaining in the absence or presence of inhibitor (compare lanes 9 and 10), whereas the control N-terminal portion of PB<sub>1</sub> (lane 6) remained relatively stable (lane 7). Thus the 205 C-terminal signal appears to be transplantable and to act independently of the N-terminal sequence which precedes it.

Together these data provide evidence that the observed instability of the 205 proteins is due to ubiquitin-targeted degradation and concur with the findings of Lawson *et al.* (1994) for a picornavirus 3C protease. We conclude, therefore, that two regions of the ORF 1a polyprotein encoded by pKT205 are potential targets for ubiquitin-mediated ATP-dependent degradation.

## Discussion

We have presented data which suggest that a region of the IBV ORF 1a polyprotein bears two degrons which result in ubiquitin modification of *in vitro*-expressed product(s) followed by degradation of the targeted protein(s) by an ATP-dependent protease present in reticulocyte lysate. This is the third reported example of a viral protein subject to turnover in this manner and involves a different virus class to the previously reported examples, in a picornavirus (Oberst *et al.*, 1993) and an alphavirus (de Groot *et al.*, 1991). In addition, the identification of this process adds to the repertoire of regulatory mechanisms potentially used by coronaviruses.

The ubiquitin-mediated ATP-dependent proteolytic pathway is a major cellular non-lysosomal protein degradation system and is responsible for modulating the levels of many cellular proteins, either for the purposes of regulation or the removal of damaged or abnormal proteins (reviewed in Gottesman & Maurizi, 1992; Ciechanover & Schwartz, 1994). The system comprises two processes, both of which display a requirement for ATP. The targeting of the protein for degradation involves modification by the covalent attachment of ubiquitin to acceptor lysine residues by certain ligase enzymes (reviewed in Hershko & Ciechanover, 1992).

While ubiquitin modification may vary in degree and may play other roles in cellular regulation, it seems that multiubiquitin chains are required most frequently to target proteins for proteolysis (reviewed in Jentsch, 1992). Degradation of the targeted protein is carried out by the 26S ATP-dependent protease, a complex of several types of subunits with a range of proteolytic activities (reviewed in Hershko & Ciechanover, 1992; Rechsteiner *et al.*, 1993). Despite the fact that the components of the two processes are becoming increasingly well characterized, the precise signals determining the metabolic stability of any given protein remain much less well understood. Several sequences have been found that contribute to the short half-life of some proteins, but no overall pattern has yet to emerge (reviewed in Ciechanover & Schwartz, 1994). One exception is the N-end rule or N-degron (Bachmair *et al.*, 1986; reviewed in Varshavsky, 1992), which relates the stability of a protein to the identity of its N-terminal amino acid, which may be stabilizing or destabilizing. This is a two part degron in that a destabilizing N-terminal amino acid promotes the multiple ubiquitination of a nearby lysine residue. Although this pathway is thought to play only a minor physiological role, it has been found to be responsible for the rapid turnover of Sindbis virus polymerase (de Groot *et al.*, 1991). Metabolic instability is a common feature of many cellular regulatory proteins and this may also apply to viral non-structural proteins such as the proteases and polymerases of positive-strand viruses. This may become apparent as more information concerning the expression patterns of these proteins accumulates.

One of the degrons identified in the 205 sequence was mapped to the predicted 3C protease domain and is most likely located towards the N terminus of the mature protein, based upon the predicted cleavage release sites. The N- and C-terminal boundaries of the 205/*Bst*XI protein are close to these cleavage sites and so this protein might be structurally similar to mature 3CLP. It is possible therefore that the instability observed is significant in terms of the virus life-cycle, although in the absence of cleavage data or *in vivo* expression data (the protein has yet to be identified in infected cells) it is not possible to determine fully the relevance of this finding to the control of coronavirus 3C expression and function. However, there is a close parallel between our observations and those of Lawson *et al.* (1994) concerning the low *in vitro* stability of EMCV 3C protease, which itself accords with the observed *in vivo* metabolic instability of several viral proteases in the 3C-like group (Oberst *et al.*, 1993). The coronavirus 3C domain may thus exhibit this characteristic feature of the 3C protease family as a conserved trait. Recent evidence in the case of HCV 229E 3C protease expression *in vivo* (Ziebuhr *et al.*, 1995)

may support this contention. Regulation of 3C protease activity through metabolic instability may be an important control process involved in coronavirus replication; this protease is likely to play a key role in the processing and maturation of ORF 1 proteins, possibly including downstream *trans* cleavages in the 1b region (Liu *et al.*, 1994) which contains the putative polymerase domain(s) (Gorbalenya *et al.*, 1989).

The potential function of the second degron identified towards the C terminus of the 205 translation product is not obvious at the present time; it lies within a region of ORF 1a with no postulated function. This degron is apparently context-independent in that its relative position within the region of the 1a protein expressed does not affect its activity. Indeed, this signal is transplantable from its native context such as to confer instability upon a normally stable heterologous protein (PB<sub>1</sub>). This property has been reported previously for the *Deg1* degradation signal located within the yeast MAT $\alpha$ 2 repressor and for the N terminus of the HPV-16 E6 protein (Chen *et al.*, 1993; Crook & Vousden, 1994). Such a degradation signal could prove potentially useful in destabilizing a protein of choice either *in cis* (as above) or *in trans* by analogy to the natural targeting of cellular p53 protein by the HPV-16 E6 protein (Crook & Vousden, 1994), although subunit preference (specificity) in the degradation of multicomplex proteins has been observed (Hochstrasser & Varshavsky, 1990). The property of a degron to function in a context-independent manner may be an important prerequisite for the control of differently processed versions of a polyprotein or to enable regulation of downstream functions whose effectors have yet to be processed from the polyprotein (possibly by 3C). It is of relevance to note here that Oberst *et al.* (1993) reported a hierarchical pattern of stability of different 3C-bearing polyprotein fragments. Thus, the two degrons identified here may both have significant impact upon the cellular levels of ORF 1 products.

Neither degron identified within the 205 protein appears to conform to the N-end rule. All the expressed products described here bear at least 4 amino acids at their N-termini that are derived from highly stable influenza virus proteins. According to the rules governing their removal (Flinta *et al.*, 1986; Ciechanover & Schwartz, 1994) it is unlikely that the N-terminal methionine residues of these proteins would be removed to reveal the destabilizing aspartate residues which follow in each case. Moreover, involvement of the N-degron in IBV 3C turnover would not be expected if mature 3C is derived in the way predicted from the proposed cleavage sites (Gorbalenya *et al.*, 1989), since the N-terminal residue would be serine, which is stabilizing according to the N-end rule. Confirmation will await identification of

3C *in vivo*, analysis of its metabolic stability and verification of the authentic cleavage sites. Currently we are generating an antiserum against the 3C domain to aid in achieving these aims.

As yet there are no indications as to how the region of the 1a polyprotein surrounding 3C is processed. The apparent lack of auto-processivity of the 205 product *in vitro* is unexpected but may be related to the residual (possibly uncleavable) protein sequence upstream of the predicted N terminus of 3C. This condition has been found to abrogate the activity of a cloned protease of hepatitis C virus (D. Rowlands, personal communication). Alternatively, it is possible that additional sequences are required for activity which lie beyond the confines of the 205 clone. Efforts to define and characterize active forms of 3C and/or other regions of ORF 1 which process *in vitro* remain in progress.

We thank Tim Crook for helpful discussion and the E6-cyclin construct, Andrea Klotzbücher for the modified ubiquitin and Ron Hay for providing MG132. We are grateful to Paul Digard for critical reading of the manuscript and Anita Hancock for manuscript preparation. This work was supported by the Biotechnology and Biological Sciences Research Council and the Ministry of Agriculture, Fisheries and Food, UK.

## References

- BACHMAIR, A., FINLEY, D. & VARSHAVSKY, A. (1986). *In vivo* half-life of a protein is a function of its amino-terminal residue. *Science* **234**, 179–186.
- BAKER, S. C., SHIEH, C.-K., SOE, L. H., CHANG, M.-F., VANNIER, D. M. & LAI, M. M. C. (1989). Identification of a domain required for autoproteolytic cleavage of murine coronavirus gene A polyprotein. *Journal of Virology* **63**, 3693–3699.
- BAKER, S. C., YOLOMORI, K., DONG, S., CARLISLE, R., GORBALENYA, A. E., KOONIN, E. V. & LAI, M. M. C. (1993). Identification of the catalytic sites of a papain-like cysteine proteinase of murine coronavirus. *Journal of Virology* **67**, 6056–6063.
- BOURNSELL, M. E. G., BROWN, T. D. K., FOULDS, I. J., GREEN, P. F., TOMLEY, F. M. & BINNS, M. M. (1987). Completion of the sequence of the genome of the coronavirus avian infectious bronchitis virus. *Journal of General Virology* **68**, 57–77.
- BRIERLEY, I., BOURNSELL, M. E. G., BINNS, M. M., BILIMORIA, B., BLOK, V. C., BROWN, T. D. K. & INGLIS, S. C. (1987). An efficient ribosomal frame-shifting signal in the polymerase-encoding region of the coronavirus IBV. *EMBO Journal* **6**, 3779–3785.
- BRIERLEY, I., DIGARD, P. & INGLIS, S. C. (1989). Characterization of an efficient coronavirus ribosomal frameshifting signal: requirement for an RNA pseudoknot. *Cell* **57**, 537–547.
- BRIERLEY, I., BOURNSELL, M. E. G., BINNS, M. M., BILIMORIA, B., ROLLEY, N. J., BROWN, T. D. K. & INGLIS, S. C. (1990). Products of the polymerase-encoding region of the coronavirus IBV. In *Coronaviruses And Their Diseases*, pp. 275–278. Edited by D. Cavanagh and T. D. K. Brown. New York: Plenum Press.
- BROWN, T. D. K. & BRIERLEY, I. (1995). The coronavirus nonstructural proteins. In *The Coronaviridae*, pp. 191–217. Edited by S. G. Siddell. New York: Plenum Press.
- CAVANAGH, D., BRIAN, D. A., ENJUANES, L., HOLMES, K. V., LAI, M. M. C., LAUDE, H., SIDDELL, S. G., SPAAN, W., TAGUCHI, F. & TALBOT, P. J. (1990). Recommendations of the coronavirus study group for the nomenclature of the structural proteins, mRNAs and genes of coronaviruses. *Virology* **176**, 306–307.
- CIECHANOVER, A. & SCHWARTZ, A. L. (1994). The ubiquitin-mediated proteolytic pathway: mechanisms of recognition of the proteolytic

- substrate and involvement in the degradation of native cellular proteins. *FASEB Journal* **8**, 182–191.
- CHEN, P., JOHNSON, P., SOMMER, T., JENTSCH, S. & HOCHSTRASSER, M. (1993). Multiple ubiquitin-conjugating enzymes participate in the *in vivo* degradation of the yeast MAT $\alpha$ 2 repressor. *Cell* **74**, 357–369.
- CRAIG, D., HOWELL, M. T., GIBBS, C. L., HUNT, T. & JACKSON, R. J. (1992). Plasmid cDNA-directed protein synthesis in a coupled eukaryotic *in vitro* transcription translation system. *Nucleic Acids Research* **20**, 4987–4995.
- CROOK, T. & VOUSDEN, K. H. (1994). Interaction of HPV E6 with p53 and associated proteins. *Biochemical Society Transactions* **22**, 52–55.
- DE GROOT, R. J., RÜMENAPF, T., KUHN, R. J., STRAUSS, E. G. & STRAUSS, J. H. (1991). Sindbis virus RNA polymerase is degraded by the N-end rule pathway. *Proceedings of the National Academy of Sciences, USA* **88**, 8967–8971.
- DENISON, M. R. & PERLMAN, S. (1986). Translation and processing of mouse hepatitis virus virion RNA in a cell free system. *Journal of Virology* **60**, 12–18.
- DENISON, M. R. & PERLMAN, S. (1987). Identification of a putative polymerase gene product in cells infected with murine coronavirus A59. *Virology* **153**, 565–568.
- DENISON, M. R., ZOLHIK, P. W., HUGHES, S. A., GIANGRECO, B., OLSEN, A. L., PERLMAN, S., LIEBOWITZ, J. L. & WEISS, S. R. (1992). Intracellular processing of the N-terminal ORF 1a proteins of the coronavirus MHV-A59 requires multiple proteolytic events. *Virology* **189**, 274–284.
- DOTTO, G. P., ENEA, V. & ZINDER, N. D. (1981). Functional analysis of bacteriophage  $\phi$ 1 intergenic region. *Virology* **114**, 463–473.
- FLINTA, C., PERSSON, B., JÖRNVALL, H. & VON HEIJNE, G. (1986). Sequence determinants of cytosolic N-terminal protein processing. *European Journal of Biochemistry* **154**, 193–196.
- GORBALENYA, A. E., KOONIN, E. V., DONCHENKO, A. P. & BLINOV, V. M. (1989). Coronavirus genome: prediction of putative functional domains in the non-structural polyproteins by comparative amino acid sequence analysis. *Nucleic Acids Research* **17**, 4847–4860.
- GOTTESMAN, S. & MAURIZI, M. R. (1992). Regulation by proteolysis: energy dependent proteases and their targets. *Microbiological Reviews* **56**, 592–621.
- HAMES, B. D. (1981). An introduction to polyacrylamide gel electrophoresis. In *Gel Electrophoresis Of Proteins – A Practical Approach*, pp. 1–91. Edited by B. D. Hames and D. Rickwood. Oxford: IRL Press.
- HEROLD, J., RAABE, T., SCHELLE-PRINZ, B. & SIDDELL, S. G. (1993). Nucleotide sequence of the human coronavirus 229E RNA polymerase locus. *Virology* **195**, 680–691.
- HERSHKO, A. & CIECHANOVER, A. (1992). The ubiquitin system for protein degradation. *Annual Review of Biochemistry* **61**, 761–807.
- HERSHKO, A., LESHINSKY, E., GANOTH, D. & HELLER, H. (1984). ATP-dependent degradation of ubiquitin–protein conjugates. *Proceedings of the National Academy of Sciences, USA* **81**, 1619–1623.
- HOCHSTRASSER, M. & VARSHAVSKY, A. (1990). *In vivo* degradation of a transcriptional regulator: the yeast  $\alpha$ 2 repressor. *Cell* **61**, 697–708.
- HOUGH, R. & RECHSTEINER, M. (1986). Ubiquitin–lysozyme conjugates. *Journal of Biological Chemistry* **261**, 2391–2399.
- JENTSCH, S. (1992). The ubiquitin-conjugation system. *Annual Review of Genetics* **26**, 179–207.
- KUNKEL, T. A. (1985). Rapid and efficient site-specific mutagenesis without phenotypic selection. *Proceedings of the National Academy of Sciences, USA* **82**, 488–492.
- LAI, M. M. C. (1990). Coronavirus: organisation, replication and expression of genome. *Annual Review of Microbiology* **44**, 303–333.
- LAWSON, T. G., GRONOS, D. L., WERNER, A., WEY, A. C., DIGEORGE, A. M., LOCKHART, J. L., WILSON, J. W. & WINTRODE, P. L. (1994). The encephalomyocarditis virus 3C protease is a substrate for the ubiquitin-mediated proteolytic system. *Journal of Biological Chemistry* **269**, 28429–28435.
- LEE, H.-J., SHIEH, C.-K., GORBALENYA, A. E., KOONIN, E. V., LA MONICA, N., TULER, J., BAGDZHADZHAN, A. & LAI, M. M. C. (1991). The complete sequence (22 kilobases) of murine coronavirus gene 1 encoding the putative proteases and RNA polymerase. *Virology* **180**, 567–582.
- LIU, D. X., BRIERLEY, I., TIBBLES, K. W. & BROWN, T. D. K. (1994). A 100 kilodalton polypeptide encoded by open reading frame (ORF) 1b of the coronavirus infectious bronchitis virus is processed by ORF 1a products. *Journal of Virology* **68**, 5772–5780.
- LU, Y., LU, X. & DENISON, M. R. (1995). Identification and characterization of a serine-like proteinase of the murine coronavirus MHV A59. *Journal of Virology* **69**, 3554–3559.
- OBERST, M. D., GOLLAN, T. J., GUPTA, M., PEURA, S. R., ZYDLEWSKI, J. D., SUDARSANAN, P. & LAWSON, T. G. (1993). The encephalomyocarditis virus 3C protease is rapidly degraded by an ATP-dependent proteolytic system in reticulocyte lysate. *Virology* **193**, 28–40.
- RECHSTEINER, M., HOFFMAN, L. & DUBIEL, W. (1993). The multicatalytic and 26S proteases. *Journal of Biological Chemistry* **268**, 6065–6068.
- RUSSEL, M., KIDD, S. & KELLEY, M. R. (1986). An improved filamentous helper phage for generating single-stranded plasmid DNA. *Gene* **45**, 333–338.
- SCHIEFFNER, M., MUNGER, K., HUIBREGTSE, J. M. & HOWLEY, P. M. (1992). Targeted degradation of the retinoblastoma protein by human papillomavirus E7–E6 fusion proteins. *EMBO Journal* **11**, 2425–2431.
- SCHIEFFNER, M., HUIBREGTSE, J. M., VIERSTRA, R. D. & HOWLEY, P. M. (1993). The HPV-16 E6 and E6-AP complex functions as a ubiquitin–protein ligase in the ubiquitination of p53. *Cell* **75**, 495–505.
- SOE, L. H., SHIEH, C.-K., BAKER, S. C., CHANG, M.-F. & LAI, M. M. C. (1987). Sequence and translation of the murine coronavirus 5-end genomic RNA reveals the N-terminal structure of the putative RNA polymerase. *Journal of Virology* **61**, 3968–3976.
- SPAAN, W., CAVANAGH, D. & HORZINEK, M. C. (1988). Coronaviruses: structure and genome expression. *Journal of General Virology* **69**, 2939–2952.
- STERN, D. F. & KENNEDY, S. J. T. (1980). Coronavirus multiplication strategy. I. Identification and characterization of virus specified RNA species to the genome. *Journal of Virology* **34**, 665–674.
- STERN, D. F. & SEFTON, B. M. (1984). Coronavirus multiplication: location of genes for virion proteins on the avian infectious bronchitis virus genome. *Journal of Virology* **50**, 22–29.
- VARSHAVSKY, A. (1992). The N-end rule. *Cell* **69**, 725–735.
- YOUNG, J. F., DESSELBERGER, U., GRAVES, P., PALESE, P., SHATZMAN, A. & ROSENBERG, M. (1983). Cloning and expression of influenza virus genes. In *The Origin of Pandemic Influenza Viruses*, pp. 129–138. Edited by W. G. Laver. Amsterdam: Elsevier.
- ZIEBUHR, J., HEROLD, J. & SIDDELL, S. G. (1995). Characterization of a human coronavirus (strain 229E) 3C-like proteinase activity. *Journal of Virology* **69**, 4331–4338.